

## Neutronic Measurements to Commission the SNS

E. B. Iverson,<sup>1</sup> B. J. Micklich,<sup>2</sup> D. V. Baxter,<sup>3</sup> R. G. Cooper,<sup>1</sup> P. D. Ferguson,<sup>1</sup>  
D. W. Freeman,<sup>1</sup> F. X. Gallmeier,<sup>1</sup> S. E. Hammons,<sup>1</sup> C. M. Lavelle,<sup>3</sup> and I. Popova<sup>1</sup>

<sup>1</sup>Spallation Neutron Source, Oak Ridge National Laboratory, Oak Ridge, TN USA

<sup>2</sup>Intense Pulsed Neutron Source, Argonne National Laboratory, Argonne, IL USA

<sup>3</sup>Indiana University Cyclotron Facility, Indiana University, Bloomington, IN, USA

### Abstract

*The commissioning of a new neutron source requires demonstration that the source is performing at a reasonable and/or satisfactory level, making neutron beams useful for neutron scattering instruments. At the SNS, we are required to meet a predefined minimum neutron production efficiency goal as part of our commissioning project. We describe the cadmium-difference foil activation-normalized time-of-flight spectral measurements we intend to make during the commissioning of the SNS facility, and the demonstration of our equipment, techniques and procedures at other pulsed neutron sources prior to SNS commissioning. These measurements are challenging because they require a degree of absolutism not usually found in spallation source characterization measurements, and also because they must be performed quickly and expediently, even though the facility will not be fully operational. At the same time, we are attempting to ensure that the equipment we will use is applicable to long-term use in the facility. Thus we have chosen equipment to be portable, so that it can be used on any beam-line within the SNS facility and at other facilities, and stable, so that it will have a reproducible absolute efficiency. These features make this apparatus appropriate for long-term beam-line characterization, monitoring, and calibration.*

### 1. Introduction

The Project Execution Plan [1] for the Spallation Neutron Source Project specifies a series of tests to demonstrate that all components of the facility are working properly to produce neutrons at a satisfactory level of performance and reach Critical Decision Four (CD4), a term used by the U.S. Department of Energy to signify project completion. One of these tests, which we refer to as the CD4 neutronics measurement (CD4n), requires that “an integrated neutron flux from the target of  $5 \times 10^{-3}$  neutrons per steradian solid angle per incident proton [be] measured viewing an ambient moderator face.” The Experimental Facilities Division Installation, Commissioning, and Operations Plan (ICOP) [2] elaborates that we will verify the neutronic effectiveness of the target, moderator, and reflector assembly by measuring the brightness of a moderator face, and that the spectral brightness will meet or exceed the spectral brightness associated with a 1-eV moderator coupling of  $5 \times 10^{-4}$  neutrons per steradian per eV per incident proton.

This measurement is complicated by a number of factors:

- There will be a strong desire to complete this measurement and transition to operational status as soon as possible, while the delivered proton beam current is quite low.
- There will be a strong desire to have the ability to re-enter the target station hot cell to perform hands-on work in the period immediately following CD4.
- Proton beam availability is likely to be less reliable than ultimately intended.
- There will be limited time and personnel available at the end of the project construction, especially given the approximately simultaneous CD4 requirement from the accelerator to deliver a single pulse of  $10^{13}$  protons through the ring to the target.

All of these factors combine to mean that the CD4n measurement will need to be done with minimal beam intensity, in a minimal amount of time, with minimal risk. Accelerator Systems personnel have indicated that they will require some days of operation at lower levels,  $10^{11}$  to  $10^{12}$  protons per pulse at 1 Hz, to complete the tuning necessary to deliver the single required  $10^{13}$ -proton pulse to the target. As the CD4n measurement is defined on a “per proton” basis, it can nominally be completed prior to the completion of the accelerator requirement, although performing the measurement will of course require a certain power level.

For various reasons, described elsewhere [3], we have decided to perform the CD4n measurement on the ARCS instrument, a chopper spectrometer with primary flight path of approximately 14 m, on beamline 18BU, viewing the ambient water moderator. The current ARCS installation schedule permits the execution of the CD4n measurement during the required time frame.

## 2. Characterization Methods

We have considered many different methods for neutron beam characterization that might be employed to demonstrate a certain level of performance of the target, moderator, and reflector assembly, and make the required CD4n measurement. The traditional method of thermal neutron foil activation, often used during operations at reactor facilities, would be somewhat difficult in this situation, as the neutron spectrum will have a high epithermal component, the (guide-enhanced) thermal component will be significantly non-Maxwellian, and the time-averaged flux levels at this stage of operations will be rather low. Epithermal foil activation might prove somewhat more effective, but would still be challenging and time-consuming, with a relatively high likelihood of failure (that is, the measurement might fail even though the beam intensity met the necessary criterion). On the other hand, intensity measurements with calibrated counting-mode neutron detectors (typical low-efficiency beam monitors) should provide a reliable means for demonstrating satisfactory neutronic performance of the SNS target station. These methods are described in detail below.

### 2.1 Beam Monitor Detectors

A calibrated low-efficiency counting detector placed in a neutron beamline will provide an estimate of the neutron flux at that location, which can be converted to provide moderator intensity. Such detectors are typically used in pulsed neutron source facilities to provide spectral distributions and intensity normalization. A low-efficiency beam monitor detector in a neutron beam such as we will use at SNS counts neutrons at a relatively constant instantaneous rate during the epithermal, or so-called  $1/E$  regime, as shown in Figure 1 for the 18BU beamline.

Given an efficiency of  $5 \times 10^{-5} \text{ \AA}^{-1}$ , a neutron beam monitor at 14 m flight path length will have an instantaneous counting rate of about 20 000 cps in the epithermal neutron energy range given the proton pulses ( $10^{13}$  protons per pulse at a maximum) envisioned during commissioning. The counting rate would peak at about 50 000 cps, well within reasonable rates for such a detector. The time-of-flight spectra from a beam monitor detector can easily be integrated over many source pulses of widely varying intensities. The detector would require a timing signal from the accelerator to begin the time-of-flight frame, and the counting system would require a signal indicating the proton current on target. Such a system would display this relatively constant counting rate up through about  $0.7 \text{ \AA}$ , or about 2.5 ms time-of-flight at 14m flightpath length. Assuming the detector could begin counting 0.5 ms following the source pulse, the resulting 2 ms at 20 000 cps results in some 40 neutron counts from a single pulse, which need not be binned more precisely given the uniform counting rate. The efficiency of the detector can easily be specified at purchase across a broad range; a  $10^{-4}$  detector would count 80 counts from that same  $10^{13}$ -proton pulse, or 8 counts from a pulse of  $10^{12}$  protons. As a further advantage, the spectrum, and thus the counting rate, is unaffected in this energy range by neutron guides (ARCS will have a neutron guide).

Considering the low power level of the pulses envisioned as part of the accelerator tuning, a detector efficiency of  $10^{-3} \text{ \AA}^{-1}$  would provide a minimum of 8 counts per  $10^{11}$ -proton pulse. We would thus measure some thousands of counts in the first hour of 1 Hz operation at  $10^{11}$  protons per pulse, providing good precision on a relatively easy measurement early in the first stages of ring commissioning, requiring no additional accelerator operations. This detector would see peak count rates of nearly 500 000 cps at  $10^{13}$  protons per pulse, however, which is not practical.

Of course, the detector would continue to count neutrons even past  $0.7 \text{ \AA}$ , and we would gain as a bonus a full neutron energy spectrum as measured from an SNS moderator; this measurement would have significant value as a rapid communication of SNS performance and operation. Furthermore, the results of this measurement are available immediately; the knowledge of success would follow within seconds of the pulse in which that success is achieved. Finally, equipment for performing this style of measurement (detailed below) will remain useful during operations at SNS. We will perform frequent neutron beam calibration and characterization measurements on most or all of the SNS neutron beamlines, and those measurements will require exactly this same equipment. These reasons combine

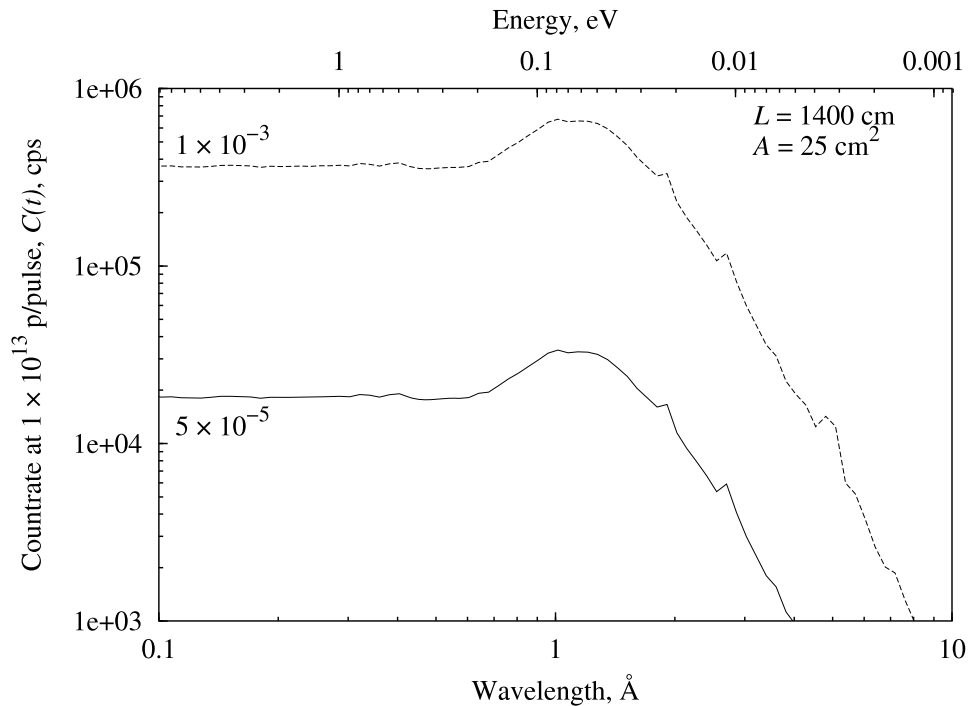


Figure 1: Instantaneous counting rates in two detectors. The upper curve is for a detector with intrinsic efficiency of  $1 \times 10^{-3} \text{ \AA}^{-1}$ , and the lower curve an efficiency of  $5 \times 10^{-5} \text{ \AA}^{-1}$ .

to make the time-of-flight measurement with a low-efficiency beam monitor detector our choice for performing the SNS CD4n measurement. Performing this measurement will require a detector system with a known, reproducible efficiency calibration. Below, we describe the methods we will use to provide this time-of-flight detector efficiency calibration and estimate its reproducibility.

## 2.2 Foil Activation

Foil activation experiments might also provide a measurement of the flux at a given location in a neutron beamline. That measured flux would give the intensity/brightness of the moderator illuminating the beamline, as required for the CD4n measurement, given certain assumptions regarding the spectral distribution of the neutron beam. The flux measurement would first involve the activation of a foil with the neutron beam, and then the spectroscopic counting of that activated foil. Given the low power levels, unpredictable operation, and desire for a timely reporting of the CD4n measurement, we have decided the foil activation is not directly practical as a means of performing the CD4n measurement.[3] However, we will employ foil activation techniques as described below to calibrate our time-of-flight beam monitor system. That said, for all the disadvantages of foil activation in this context, it would require no equipment beyond what we already have, and may prove a useful backup experiment should other equipment fail.

## 2.3 Demonstration

Our method of measurement must be demonstrated, with the equipment and procedures to be used during commissioning, prior to that commissioning. Such demonstration and testing is especially vital given the low-fluence requirements for making the CD4n measurement, as well as the time-sensitivity and overall importance of a successful measurement. As SNS will obviously not have neutron beams available at that point, such testing must take place elsewhere. Coincidentally, the neutron intensity per pulse at IPNS (operating at  $15 \mu\text{A}$ ) is comparable to that of SNS at the  $10^{12}$  protons-per-pulse level. Therefore, we chose to demonstrate the measurements and calibrate the detectors on IPNS beamlines. At the same time, such activities characterize those IPNS beamlines, a topic of interest to IPNS, reported on elsewhere in these proceedings.[4] The goals of this demonstration are

- to determine the detector system efficiency,
- to determine the reproducibility of the detector system efficiency,

- to develop and demonstrate the procedure for use in making the CD4n measurement,
- to develop the data acquisition software to perform the measurement and rapidly report its results, and
- to verify the ongoing functionality of the detector system.

Additionally, with this demonstration we will

- develop and refine the techniques we will use for beam characterization at SNS on an ongoing basis,
- explore the use of these techniques on guided, filtered, chopped, and otherwise modified neutron beams, and
- provide such characterizations for the beamlines IPNS on which we perform the demonstration.

### 3. Efficiency Calibration

The neutron beam intensity emitted from a moderator face, normalized by the accelerator beam current, corresponds to what in optics terminology is a normalized “luminous intensity.” This intensity is related to a measured flux;

$$i(E) = \frac{L^2}{I} \phi(E)|_L, \quad (3.1)$$

where  $\phi(E)$  is the time-averaged flux per unit energy at a distance  $L$  far from the moderator face, and  $I$  is the time-averaged accelerator beam current. In general, the use of the intensity rather than flux as a metric permits the performance of the moderator to be specified independently from the length of the flight path. The units of  $i(E)$  are then neutrons per steradian per second per electron-Volt per micro-ampere (or neutrons per steradian per second per eV per proton). The commonly quoted measure of moderator coupling effectiveness is this quantity, evaluated at 1 eV,  $i(E)|_{1 \text{ eV}}$ , referred to in the ICOP. The official CD4n quantity described above as specified in the Project Execution Plan is the integral of  $i(E)$  over all energies.

If the intensity  $i(E)$  is multiplied by  $E$ , the resulting quantity is proportional to the normalized counting rate seen in a thin  $1/v$  detector placed at a distance  $L$  from the moderator surface, scaled by a factor which is independent of neutron energy. Thus  $E \times i(E)$  is easily compared to a time-of-flight beam intensity measurement.

A combination of foil activation and time-of-flight spectral measurements can provide absolutely normalized intensities for a neutron beam. A low efficiency  $1/v$  detector operated in a counting mode records the intensity of the neutron beam, while a cadmium-difference foil activation measurement (performed at the same time) provides the scale factor for the detector efficiency, and thus normalizes the detector output to an absolute scale. Given the time-averaged counting rate per unit time-of-flight  $C(E)$  as a function of energy  $E$ , the energy-differential flux  $\phi(E)$  at the detector location can be found from

$$\phi_D(E) = \frac{C(E) - B}{EK'}. \quad (3.2)$$

Here  $B$  is a constant background counting rate and  $K'$  is an absolute detector efficiency, dependent on the detector itself, the area of the neutron beam, and the length of the neutron flight path, but independent of energy. We can modify Equation 3.2 to relate the flux at a foil irradiation position (beam-line length  $L_F$ ) to the net counting rate at the detector position (beam-line length  $L_D$ ),

$$\phi_F(E) = \frac{C(E) - B}{EK}, \quad (3.3)$$

where  $K$  is a scaled absolute efficiency

$$K = K' \frac{L_F^2}{L_D^2}. \quad (3.4)$$

The value of the scaled absolute efficiency  $K$  can be shown [5] to be

$$K = \frac{2N_c N_b}{N_c \alpha_b (1 - \gamma(t_1)) - N_b \alpha_c} \int_{t_1}^{t_2} \left(1 - e^{-\Sigma_{Cd}(t)s} - \gamma(t_1)\right) \sigma_{\text{foil}}(t) \frac{C(t) - B}{t} dt. \quad (3.5)$$

where  $N_{b,c}$  represent the number of atoms available for activation in the bare and covered activation foils respectively,  $\alpha_{b,c}$  the saturation activity of the foils,  $\Sigma_{Cd}$  the removal cross section of the cadmium cover of thickness  $s$ ,  $\sigma_{\text{foil}}$  the

activation cross section of the foil, and  $t_1$  and  $t_2$  define the time-of-flight range over which the count rate data  $C(t)$  are available. This time-of-flight range should cover an energy range which includes the majority of the activation caused by the neutron beam (i.e., all of the thermal energy range as well as any low-lying resonances). The dimensionless parameter  $\gamma(t_1)$  corrects for the imperfect transmission of the cadmium cover at high energies, and is discussed in detail below. The absolute efficiency  $K'$  is related to the intrinsic detector efficiency  $k$ ,

$$k = K' \frac{L_D m}{2A h}, \quad (3.6)$$

where  $h$  is Planck's constant,  $m$  is the mass of the neutron,  $A$  is the area of the beam, and  $L_D$  is the length of the flight path.

The flux as a function of energy at the sample position can then be calculated using the counting rates  $C(t)$  taken during the activation experiment and from Equation 3.3. The cadmium-difference technique thus permits normalization of the spectrum to take place even without monitor data at higher neutron energies, corresponding to time-of-flight less than  $t_1$ , where recovery from the initial prompt radiation pulse distorts the response of the detector, and where resonance effects complicate the interpretation of activation data.

### 3.1 Cadmium Cover Correction

The parameter  $\gamma$  accounts for the imperfect transparency of the cadmium cover at energies above the energy corresponding to time-of-flight  $t_1$ ; that is, energies for which time-of-flight data are not available. Given an energy  $E_1$  corresponding to the lower time-of-flight limit  $t_1$ , the quantity  $1 - \gamma$  is the ratio of the activities of covered and bare foils exposed to a neutron flux containing only energies greater than  $E_1$ . If cadmium were perfectly transparent at these energies, then the activities would be equal and  $\gamma$  would be zero.

If we consider the cadmium cover and the activation foil to be perfectly absorbing materials with no scattering cross section, then  $\gamma$  can be defined mathematically as

$$\gamma(E_1) = \frac{\int_{E_1}^{\infty} (1 - e^{-\Sigma_{Cd}(E)s}) \sigma_{\text{foil}}(E) \phi(E) dE}{\int_{E_1}^{\infty} \sigma_{\text{foil}}(E) \phi(E) dE}, \quad (3.7)$$

that is,  $\gamma(E_1)$  is the attenuation of a cadmium cover, averaged over the neutron flux spectrum above energy  $E_1$  as weighted by the activation cross section of the foil behind the cadmium cover.

## 4. Activation Foil Materials

An uncertainty analysis of Equation 3.5 indicates that the calculation of  $K$  will be quite sensitive when the bare and covered foil activities are approximately equal. In spallation sources, neutron beams are typically quite undermoderated, and previous experience at IPNS [6] with gold activation foils indicated that the bare and covered foil activities are indeed approximately equal. With that in mind, we considered different foil materials, and have determined that dysprosium may offer significant advantages, because it has a fairly high thermal neutron absorption cross section and a low resonance integral.

Dysprosium is an interesting candidate foil material because  $^{164}\text{Dy}$ , which has an abundance of 28.18%, is a pure  $1/v$  absorber up to 100 keV. Thus a cadmium-difference activation measurement should result in a larger relative activity difference between the covered and bare foils. The  $^{164}\text{Dy}(n,\gamma)^{165}\text{Dy}$  reaction yields a gamma ray of 361.7 keV, but this energy has a branching ratio (photons emitted per decay) of only 0.0084. Other gamma rays have higher branching ratios, particularly the 94.7-keV (0.03578 branching ratio) and the 46.77 and 47.55-keV (0.072 total branching ratio) gamma rays. We also explored alternatives to gold activation foils because, even though gold is the standard activation material for a cadmium-difference experiment, we were concerned that there is a potential problem with the use of gold activation foils in a spallation source environment. Natural gold consists of 100%  $^{197}\text{Au}$ , an isotope with a fairly large thermal neutron activation cross section (approximately 100 b), leading to an activation product ( $^{198}\text{Au}$ ) with a very favorable half-life (2.7 days) producing an abundant (96% branching ratio) gamma ray with a reasonable energy (411.8 keV). One potential source of systematic error in a spallation source environment, however, arises from the 425.6-keV gamma rays produced by the decay of  $^{196}\text{Au}$ . This isotope is formed in the reaction  $^{197}\text{Au}(n,2n)$  by neutrons in the beam having energies greater than the reaction threshold energy of 8.114 MeV. These two gamma rays are too close in energy to be effectively distinguished from each other using a sodium iodide detector, and the half-life of 6.2 days is not sufficiently different from the  $^{198}\text{Au}$  half-life to easily separate the activities. As part of our measurement campaign, we performed high-resolution spectroscopy on gold foils irradiated at IPNS, and found no significant interference from this reaction. These measurements are described elsewhere in these proceedings.[4]

Even though these measurements indicate that the  $^{197}\text{Au}(n,2n)^{196}\text{Au}$  reaction does not interfere, we are still interested in exploring the dysprosium foil options because of the experimental precision issues described above.

#### 4.1 Cadmium Correction Factor for Different Foils

The quantity  $\gamma$  might be estimated analytically for different foil materials by evaluating the integrals in Equation 3.7 using estimates of the fast neutron spectrum and tabulated cross section information for the activation foil and the cadmium cover. In doing so, we determined a value for  $\gamma(E_1)$  for a gold activation foil of approximately 0.042–0.045, for energies  $10 < E_1 < 50$  eV, depending on the exact shape of the fast spectrum we used. Because we were evaluating fast and high-energy neutron spectra in SNS beamlines for other purposes at that time, we also chose to estimate  $\gamma(E_1)$  by simulation techniques using MCNPX. This calculation initially seemed quite simple, but we were very surprised to find that our first results, using relatively idealized foil and cover geometries, indicated that the parameter  $\gamma$  would be negative—that is, that the covered foil would be slightly more activated than would the uncovered foil if thermal neutrons were not considered! Although the value  $\gamma$  we found using this idealized-geometry simulation was still fairly small, approximately -0.01, the change from 0.04 could result in calculated effective efficiencies  $K$  (and thus intrinsic efficiencies  $k$ ) that differed by nearly a factor of two. Further investigation, using more realistic geometric models of a cadmium-difference foil activation measurement, resulted in values that are positive as expected, but much smaller than had been indicated by the analytical calculation. The results of these calculations are shown in Figure 2. The first line (labeled “Unfiltered”) shows  $\gamma$  for the prototypical case appropriate for use in our

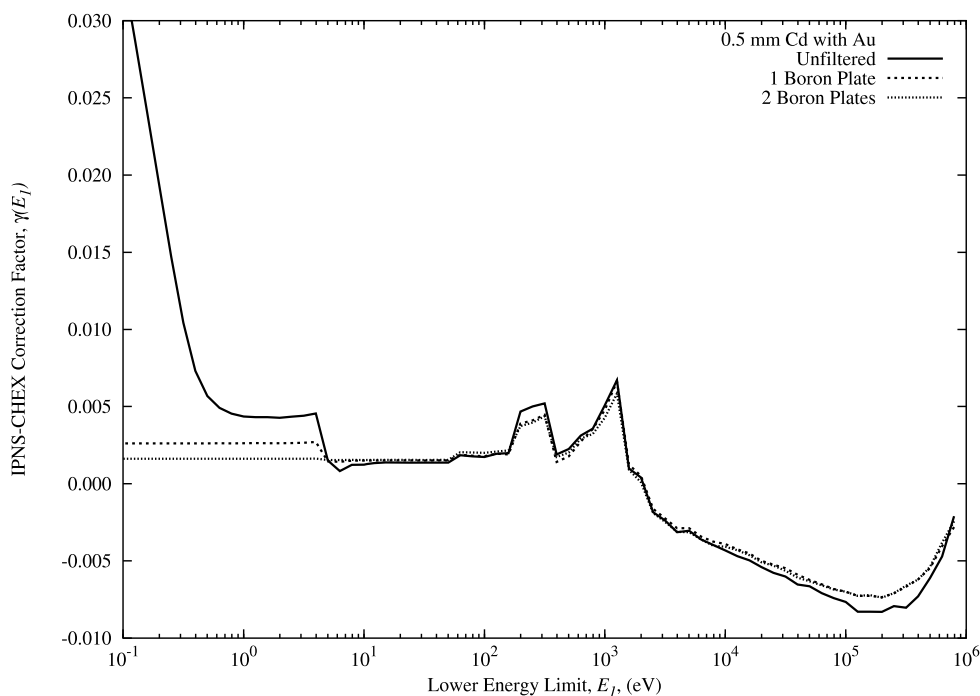


Figure 2: The  $\gamma$  parameter as estimated by simulation.

activation measurements. The remaining lines show simulations with boron filters as described below. We attribute the enhancement of the activation in the covered foil to scattered neutrons from the cadmium cover crossing the activation foil at angles significantly different from that of the primary beam, resulting in a significantly increased effective activation foil thickness.

Given that different methods of calculating the parameter  $\gamma(E_1)$  yielded such remarkably different results, we attempted to measure the quantity by using a thick boron filter over both cadmium-covered and otherwise bare foils. This boron cover should eliminate the neutrons below energy  $E_1$ , approximating the value of  $\gamma(E_1)$  as

$$\gamma(E_1) \approx \gamma(0) = 1 - \frac{\alpha_c}{\alpha_b}. \quad (4.8)$$

## 5. Equipment

We chose the equipment we will use to perform the CD4n measurement in such a way that it will also be useful for routine beam characterization activities during SNS operations. For detectors, we chose two commercial pancake-style beam monitors from LND, Inc. These detectors have active areas six inches (15 cm) in diameter, large enough to fully intercept the largest neutron beams foreseen on SNS scattering instruments. We purchased two detectors, both filled with  $^3\text{He}$  in argon. The partial pressure of  $^3\text{He}$  was specified such that the efficiency of one of the detectors (detector 2238) would be  $5 \times 10^{-5} \text{ \AA}^{-1}$ , and the other (detector 2237) would be  $1 \times 10^{-3} \text{ \AA}^{-1}$ . Thus the lower-efficiency detector should have a reasonable 20 000 cps countrate for the highest-charge accelerator pulse we might anticipate during commissioning, and the higher-efficiency detector should have a practical 4 000 cps countrate for the lowest-charge commissioning pulse. The detectors are combined with commercial preamplifiers, shaping amplifiers, high-voltage power supplies, and PCI-based multi-channel scaler cards for use as a time-of-flight counting system. The assembled system is quite portable, consisting of the detectors, preamps, a single (full) mini-NIM bin, and a desktop computer containing the PCI-based MCS cards. A block diagram of the system appears in Figure 3.

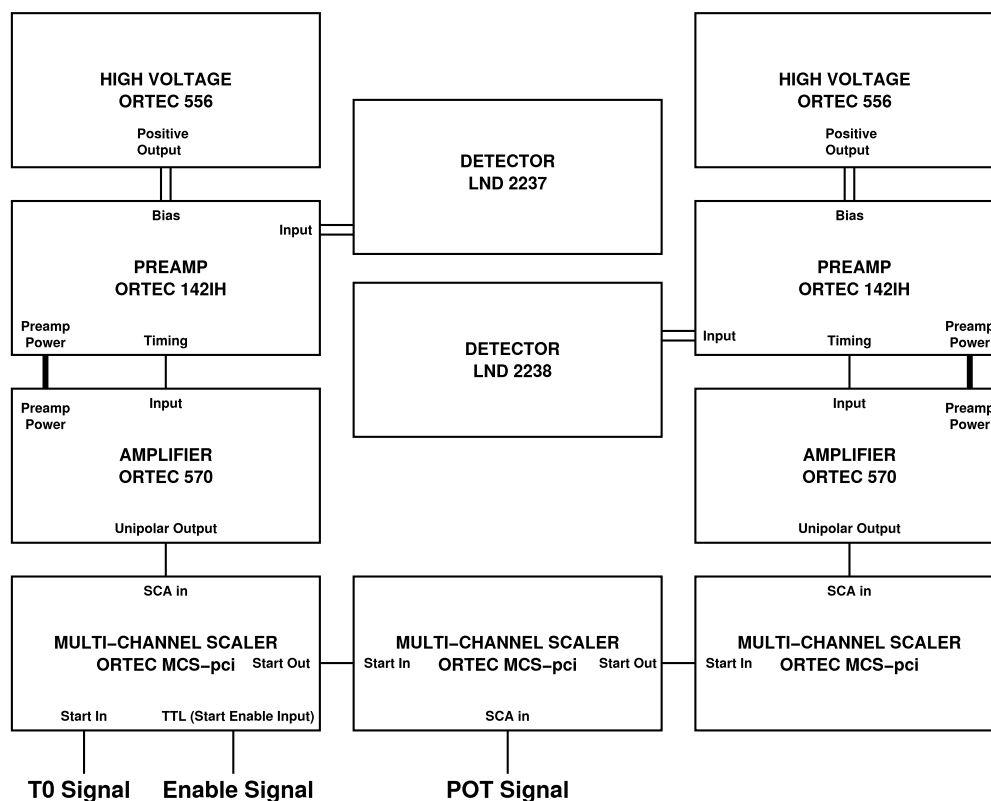


Figure 3: Data acquisition system for CD4n apparatus.

## 6. Results

We measured the absolute spectral intensities of the neutron beams on several IPNS beam-lines. A more complete description of these measurements appears elsewhere in these proceedings. [4] In the process of performing these measurements, we characterized the CD4n detector efficiency multiple times, in significantly different beam environments. Further, we have measured the CD4n detector efficiency at a continuous, monochromatic beam at the HFIR reactor. We find that we can reproduce similar values for the absolute detector efficiency in significantly different spectral situations, but that neutron guides can introduce significant systematic errors into these methods.

### 6.1 Detector Efficiencies

In experiments described elsewhere in these proceedings, we simultaneously activated gold and dysprosium foils and measured time-of-flight neutron spectra, analyzing the resulting data using the methods described above. The

intrinsic detector efficiencies  $k$  resulting from these measurements appear in Table 1. We experienced difficulties

Table 1: Efficiency measured for detector 2238, for which the specified efficiency is  $5 \times 10^{-5} \text{ \AA}^{-1}$ .

Guide	Measurement Date	Beamline	Calibration Method	Efficiency $k$ ( $\text{\AA}^{-1}$ )	Uncertainty (%)
None	12/08/2004	IPNS-CHEX	Au-foil	$6.8 \times 10^{-5}$	30
None	02/03/2005	HFIR-H2DS	Thick Det.	$7.5 \times 10^{-5}$	1
None	03/09/2005	IPNS-HRMECS	Au-foil	$7.5 \times 10^{-5}$	25
Straight	12/09/2004	IPNS-GPPD	Au-foil	$6.3 \times 10^{-5}$	23
Funnel	03/08/2005	IPNS-QENS	Au-foil	$8.9 \times 10^{-5}$	17

determining the counting efficiency of our spectroscopy system at the low energies associated with the more abundant dysprosium lines. Dysprosium foils were counted with the same spectroscopy system as the gold foils and analyzed in a parallel manner, but the activities were not high enough to produce meaningful results. The results shown here are based on the gold foil activation results.

The first two measurements at IPNS (on CHEX and HRMECS) used neutron beams without guides. As indicated in the table, we were able to achieve results which were consistent with each other, as well as with a separate measurement comparing the low-efficiency beam monitor detector to a high-efficiency (black) detector at a monochromated HFIR beamline used for SNS detector development. We emphasize that these three experiments were done at significantly different times, in significantly different beam spectra. The CHEX beam is a fairly standard beam from a liquid methane moderator. The HRMECS beam was modified by an operating IPNS-style (vertical axis) T0 chopper, significantly altering the spectrum from a solid methane moderator. The HFIR beam is a continuous, monochromated 4.25  $\text{\AA}$  beam. We feel these results indicate that our methods produce sound, reproducible detector system efficiencies.

The last two lines in Table 1 represent measurements on guided neutron beams. The efficiencies indicated are more dispersed than for the unguided beams. We believe this to be caused by the fact that guided beams can have significantly different beam sizes (that is, transverse extents) as a function of wavelength. While the detector still intercepts the larger footprint of the long-wavelength neutrons, those neutrons are spread out in such a way that the flux per unit area (responsible for the foil activation) is significantly lower than the measured spectra would indicate. That said, the efficiencies determined are still quite similar, well within the experimental errors quoted. Using the values from Table 1, we find that our detector system has an intrinsic efficiency  $k = 7.5 \times 10^{-5} \text{ \AA}^{-1}$ , and that this value is reproducible with about a 10% deviation ( $1\sigma$ ). Again, we feel that this number is quite robust, given its reproducibility across multiple setups, spectra, and situations.

Figure 4 shows the time-of-flight spectrum recorded during the CHEX measurement. Two things are immediately apparent from the graph. First, the detector system has apparently recovered from the after-effects of the prompt flash by approximately 200  $\mu\text{s}$  after the proton pulse, providing a lower limit to the effective wavelength range over which the detector can reasonably operate (for this beamline). This time is significantly earlier than what we estimated we would require for the CD4n measurement (500  $\mu\text{s}$ ). Second, the system clearly operates satisfactorily at instantaneous counting rates of approximately 10 000 cps, again satisfying our requirements as detailed above.

Simultaneous measurements on HRMECS with both CD4n detectors (detector 2238 with nominal efficiency of  $5 \times 10^{-5} \text{ \AA}^{-1}$  and 2237 with nominal efficiency of  $1 \times 10^{-3} \text{ \AA}^{-1}$ ), indicated significant problems with the countrates for the higher efficiency detector, as shown in Figure 5. We are investigating other preamplifier choices to address this problem. Our initial choice for preamplifier was the ORTEC 142PC, and we found that it required much more recovery time after the prompt flash than did our second choice, the ORTEC 142IH. The data shown here were taken using the ORTEC 142IH. We are also exploring other detector configurations and gas fills in an effort to reduce the effects of the prompt flash, which was significantly worse in the HRMECS measurements. Similar measurements with a smaller beam monitor detector with additional guard wires, and with a nitrogen fill gas rather than argon displayed a much reduced prompt flash effect. We cannot yet explain the difference in recovery times from the prompt flash for the same detector in the CHEX and HRMECS measurements.

## 6.2 Measuring the Cadmium Correction Factor

Unfortunately, our first attempt to measure the  $\gamma$  parameter was not particularly successful. Six foils, three gold and three dysprosium, were placed in the CHEX beamline at IPNS and irradiated for a period of six days. For each type of foil, there was one bare foil, one covered by 0.5 mm of cadmium (the thickness used in our cadmium-difference irradiations), and one covered by 2 mm cadmium. All foils were placed behind a ceramic plate of approximate



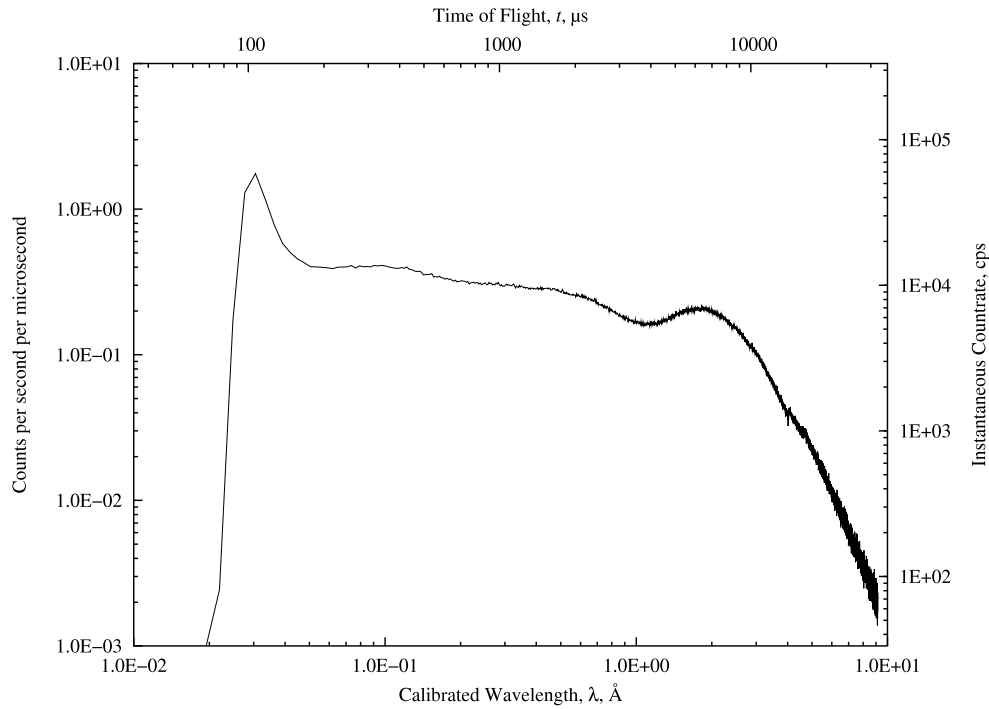


Figure 4: Time-of-flight spectrum for CHEX measurement.

Table 2: Results from  $\gamma$  measurement. The uncertainties listed reflect only the uncertainties in the spectroscopy of the activated foils.

Foil Type	Cover	Cover Thickness (mm)	Foil Mass (mg)	$\alpha_\infty$ (Bq/mg)	Uncertainty (%)	$\gamma$
Au	none	n/a	18.68	14.94	0.12	-
Au	Cd	0.5	20.16	14.48	0.10	+0.031
Au	Cd	2.0	19.94	14.79	0.09	+0.0095
Dy	none	n/a	11.75	1.69	8.87	-
Dy	Cd	0.5	11.75	1.70	12.2	-0.010
Dy	Cd	2.0	11.75	1.88	26.5	-0.12

composition 75% B<sub>4</sub>C and 25% SiC having total thickness 0.635 cm. The plate reduced the amount of activation due to low-energy neutrons and allowed us to focus on the effects of neutrons having energy greater than a few eV. Table 2 shows the saturation activities resulting from this foil irradiation. The gold foil results indicate that  $\gamma$  is positive with a value of perhaps a few percent for a 0.5-mm Cd cover. However, as shown in Figure 2, a single boron plate inadequately screened the 4.9 eV resonance in the gold foil. Thus the measured activity ratio  $\gamma(0)$  should not be expected to match the required value  $\gamma(E_1)$ . We intend to repeat the experiment with a thicker boron filter. As also shown in Figure 2, a boron filter of 12.7 mm will adequately screen the gold resonance. An additional source of difficulty in the  $\gamma$  measurement is that eliminating all thermal neutrons from a cadmium-difference gold foil activation measurement on these beamlines results in foils with nearly identical activities. The difference between the resulting two nearly identical activities has far higher relative uncertainty than do the activities themselves.

The dysprosium foil data are inconclusive, since the observed changes are significantly less than the uncertainty in counting statistics, which is partially due to the small mass of dysprosium foils used. However, the peak area uncertainties listed in Table 2 are only one contribution to the uncertainty in the quantity  $\gamma$ . As we remain unsatisfied with our attempts to measure the  $\gamma$ , we have used  $\gamma = 0.0014$  in our analysis, which comes from the Monte Carlo modeling described above. This value is appropriate for use with energy cutoffs between 5 and 50 eV.

We note in passing that the use of the CD4n-system detectors as a portable beam monitoring system provides

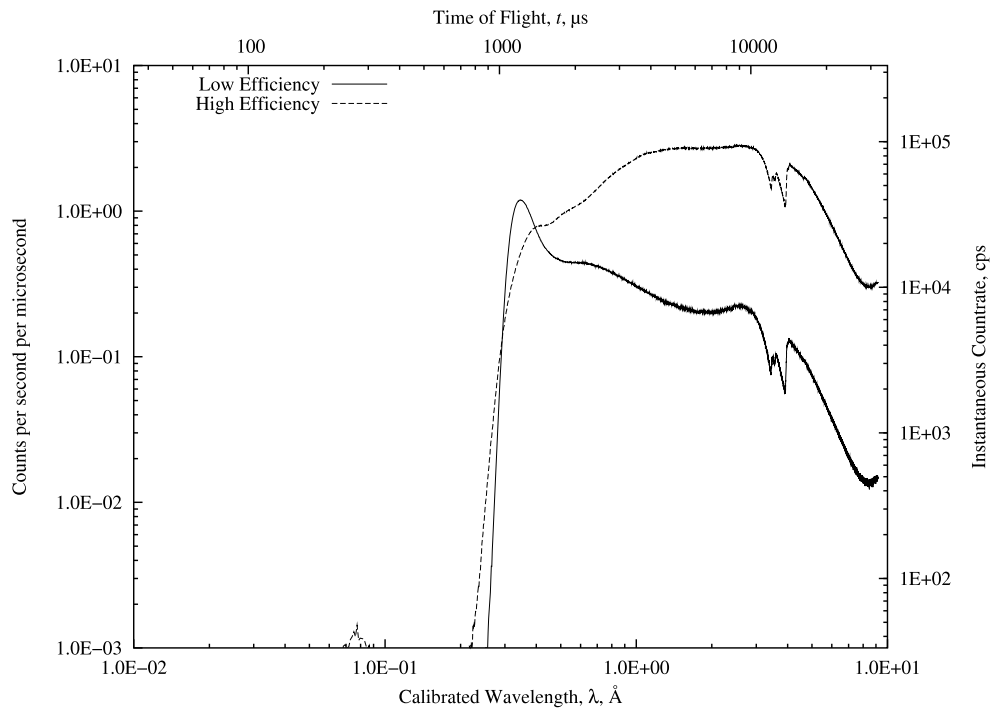


Figure 5: Time-of-flight spectra for HRMECS measurement with detectors of different efficiencies.

one additional operational challenge. Even the relatively low thermal fluxes coming from undermoderated, unguided beams at IPNS resulted in activities in the aluminum detector windows such that the detectors could not be released to non-radiation areas for several days following the irradiation period.

Of course, the efficiency of the detector system is not the eventual purpose of this measurement. Using the efficiencies we obtain above, we find that the moderator coupling on the CHEX beamline is  $1.9 \times 10^{-3}$  neutrons per steradian per eV per incident proton. The “CD4n units” value is  $3.9 \times 10^{-2}$  neutrons per steradian per proton.

## 7. Conclusions

We have demonstrated the procedure we will use to perform the SNS CD4 neutronics measurement, which will verify that the SNS target station is performing according to pre-defined expectations. The completion of this measurement, as well as similar measurements of accelerator performance, will define the end of SNS construction and the beginning of SNS operation.

We will use calibrated low-efficiency beam monitor detectors in an SNS neutron beam to perform this measurement. We have assembled the equipment to be used and tested it on IPNS beamlines. During these tests, we have successfully calibrated one of the two detectors, and we have demonstrated that this efficiency is satisfactorily reproducible across significantly different setups, at significantly different times, and in significantly different beam spectra. We have identified the challenges remaining to be met for reliable performance of the CD4n measurement;

- We must improve the recovery time of the detectors from the effects of the prompt flash.
- We must demonstrate satisfactory performance of the higher efficiency detector.
- We must measure the intrinsic efficiency of the higher efficiency detector.
- We must develop a software data acquisition interface that will allow more rapid availability of results.

Finally, we have approximately one year remaining before the CD4n measurement is to be performed. We must assure that the equipment remains functional and calibrated throughout that time period.

## Acknowledgements

We gratefully acknowledge the help provided by the instrument scientists and scientific associates on the respective instruments and by the IPNS data acquisition staff. This work was supported by the U. S. Department of Energy under contracts W-31-109-ENG-38 and DE-AC05-00OR22725 and by the National Science Foundation under grant DMR-0220560.

## References

- [1] T. Mason, “Spallation Neutron Source Project Execution Plan.” SNS 102010100PN0001-R03, 2002.
- [2] J. Forester, “Experimental Facilities Division Installation, Commissioning, and Operations Plan.” SNS-110040000-PN0001-R00, 2002.
- [3] E. B. Iverson, “Measuring the neutronic performance of the SNS for CD-4,” Tech. Rep. SNS-110040300-TR0004-R00, Oak Ridge National Laboratory, 2004.
- [4] B. J. Micklich, E. B. Iverson, D. W. Freeman, R. G. Cooper, P. D. Ferguson, F. X. Gallmeier, S. E. Hammons, I. Popova, D. V. Baxter, and C. H. Lavelle, “Spectral intensity benchmarking on IPNS beamlines,” in *Proceedings of ICANS-XVII, the Seventeenth Meeting of the International Collaboration on Advanced Neutron Sources*, 2005.
- [5] E. B. Iverson and J. M. Carpenter, “Cryogenic moderators on pulsed neutron sources: Simulations and measurements,” in *Proceedings of the 2nd International Topical Meeting on Nuclear Applications of Accelerator Technology, AccApp '98*, pp. 46–58, American Nuclear Society, September 1998.
- [6] E. B. Iverson, J. M. Carpenter, and E. J. Hill, “Absolute beam intensity measurements at the Intense Pulsed Neutron Source,” in *Proceedings of the International Workshop on Cold Moderators for Pulsed Neutron Sources* (J. M. Carpenter and E. B. Iverson, eds.), pp. 283–292, OECD, 1998.